

# ChemComm

Accepted Manuscript



This is an *Accepted Manuscript*, which has been through the Royal Society of Chemistry peer review process and has been accepted for publication.

*Accepted Manuscripts* are published online shortly after acceptance, before technical editing, formatting and proof reading. Using this free service, authors can make their results available to the community, in citable form, before we publish the edited article. We will replace this *Accepted Manuscript* with the edited and formatted *Advance Article* as soon as it is available.

You can find more information about *Accepted Manuscripts* in the [Information for Authors](#).

Please note that technical editing may introduce minor changes to the text and/or graphics, which may alter content. The journal's standard [Terms & Conditions](#) and the [Ethical guidelines](#) still apply. In no event shall the Royal Society of Chemistry be held responsible for any errors or omissions in this *Accepted Manuscript* or any consequences arising from the use of any information it contains.

## COMMUNICATION

Cite this: DOI:

A Stable Fluorinated and Alkylated Lithium Malonatoborate Salt

10.1039/x0xx00000x

Received 00th January 2012,

for Lithium Ion Battery Application

Accepted 00th January 2012

DOI: 10.1039/x0xx00000x

Shun Wan <sup>a</sup>, Xueguang Jiang <sup>b</sup>, Bingkun Guo <sup>a</sup>, Sheng Dai <sup>a, b</sup>, Xiao-Guang

www.rsc.org/

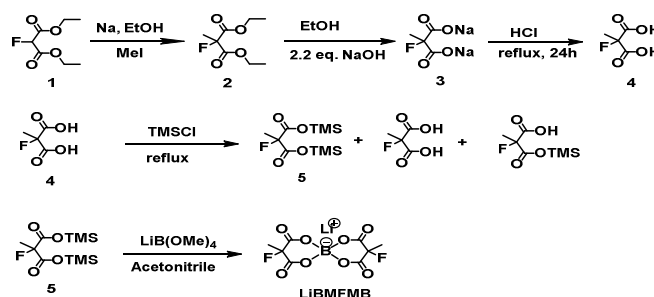
Sun <sup>a, \*</sup>

**A new fluorinated and alkylated lithium malonatoborate salt, lithium bis(2-methyl-2-fluoromalonato)borate (LiBMFMB), has been synthesized for lithium ion battery application. A 0.8 M LiBMFMB solution is obtained in a mixture of ethylene carbonate (EC) and ethyl methyl carbonate (EMC) (1:2 by wt.). The new LiBMFMB based electrolyte exhibits good cycling stability and rate capability in LiNi<sub>0.5</sub>Mn<sub>1.5</sub>O<sub>4</sub> and graphite based half-cells.**

Lithium orthoborate salts have been intensively studied during the last two decades because of their distinct thermal stability and their potential of replacing commercial LiPF<sub>6</sub>, which has low chemical and thermal stability.<sup>1-7</sup> One particular member is lithium bis(oxalato)borate (LiBOB), which showed significantly improved thermal stability over LiPF<sub>6</sub> at 70 °C.<sup>8</sup> Also a claimed unique feature of LiBOB was the participation in the solid electrolyte interphase (SEI) formation by the BOB<sup>-</sup> anion, which allowed the use of pure propylene carbonate (PC) based electrolyte in graphite electrode based cells without causing solvent co-intercalation and graphite exfoliation.<sup>9</sup> The reduction process of LiBOB at *ca.* 1.7 V vs. Li/Li<sup>+</sup> was believed to be related to the oxalate moiety that affected the initial irreversible capacity.<sup>10, 11</sup> However, it was still difficult to determine whether the oxalate was originated from the BOB anion or from an independent oxalate impurity in the LiBOB electrolyte.<sup>11</sup>

As compared to LiBOB, its close analog salt, lithium bis(malonato)borate (LiBMB) has rarely been studied, mainly due to its insolubility in common carbonate solvents.<sup>6</sup> Fortunately, the two hydrogens on the C-2 position of the BMB anion can be modified to improve the salt solubility in organic solvents. As a result, several C-2 modified LiBMB salts have been synthesized for application in lithium ion batteries.<sup>12-18</sup> Recently, we have synthesized a new C-2 modified LiBMB, lithium bis(fluoromalonato)borate (LiBFMB), which had higher oxidation stability than LiBOB, was soluble in carbonate mixtures and exhibited good cycling performance in 5.0 V LiNi<sub>0.5</sub>Mn<sub>1.5</sub>O<sub>4</sub> based half-cells.<sup>19</sup> It was also found that the BFMB anion based ionic liquids could be used as additives, at a concentration as low as 2 wt%, in 1.0 M LiPF<sub>6</sub>/PC electrolyte to afford its compatibility with graphite electrode without causing exfoliation.<sup>20</sup> However, the C-2 hydrogen in the BFMB anion is

acidic because it is adjacent to both fluorine and carbonyl groups. Therefore, the long term stability of LiBFMB against both reduction and oxidation still needs to be improved. Herein, we report the synthesis and characterization of a new stable C-2 modified LiBMB salt, lithium bis(2-methyl-2-fluoromalonato)borate (LiBMFMB). This new salt exhibits good cell performance in LiNi<sub>0.5</sub>Mn<sub>1.5</sub>O<sub>4</sub> and graphite electrode based half-cells.



Scheme 1. Synthesis of LiBMFMB

The synthesis of LiBMFMB is illustrated in **Scheme 1** with detailed experimental procedure described in the electronic supplementary information (ESI). The key intermediate, bis(trimethylsilyl) 2-methyl-2-fluoromalonate, was synthesized by using trimethylsilyl chloride as both reactant and solvent. To push the esterification as complete as possible, the unreacted trimethylsilyl chloride and the trapped HCl were removed under vacuum after overnight reaction and were replenished with fresh trimethylsilyl chloride. Such process was repeated several times until the <sup>1</sup>H NMR spectra showed that only trace amount of the starting acid was left. After repeated distillation, the final product still contains the mixture of trace starting acid, monotrimethylsilyl 2-methyl-2-fluoromalonate, and bis(trimethylsilyl) 2-methyl-2-fluoromalonate. Fortunately, during the synthesis of LiBMFMB, the reaction product from monotrimethylsilyl 2-methyl-2-fluoromalonate and lithium tetramethylborate was not soluble in anhydrous acetonitrile and could be easily removed by filtration. Also, the trace amount of unreacted starting acid could be easily removed by repeated washing

with dry ether in which LiBMFMB was not soluble. Finally, high purity LiBMFMB was obtained by repeated recrystallization from anhydrous acetonitrile and toluene. As shown in Fig. S1, LiBMFMB is stable up to 230°C under nitrogen atmosphere.

To remove the residual solvent trapped in the salt, calculated amount of LiBMFMB was dissolved in EC/dimethyl carbonate (DMC) (1/2, by wt.) in an argon-filled glove box.<sup>19</sup> The solution was then taken out the glove box and was subjected to a high vacuum of 10 mtorr at 50 °C for overnight, after which only EC was left. Finally, based on the integration of the <sup>1</sup>H NMR signals for LiBMFMB and EC, calculated amounts of EC and EMC were subsequently added to prepare the 0.8 M LiBMFMB solution in EC-EMC (1/2 by wt.).

Fig. 1 shows the temperature dependence of the ionic conductivity of 0.8 M LiBMFMB in EC-EMC (1:2 by wt.). For comparison, the ionic conductivities of 1.0 M solutions of both LiPF<sub>6</sub> and LiBOB in the same solvent mixture were also measured. As shown in Fig. 1, the ionic conductivity follows the order of LiPF<sub>6</sub> > LiBOB > LiBMFMB, which is similar to previously observed trend for LiPF<sub>6</sub> and LiBOB.<sup>19, 21</sup> The lower ionic conductivity of LiBMFMB than that of LiBOB is mainly due to its lower ion mobility, as the former anion is much larger and heavier than that of the latter anion.<sup>19</sup> At 25 °C, the ionic conductivity of 0.8 M LiBMFMB is  $2.4 \times 10^{-3} \text{ S cm}^{-1}$ , which is good for application in lithium ion batteries.

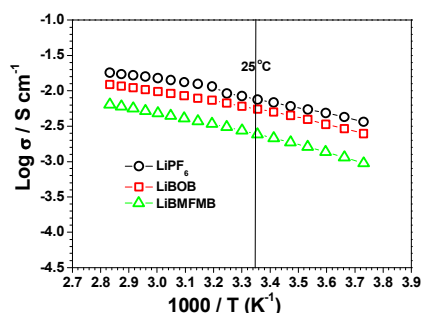


**Fig. 1.** The temperature dependence of ionic conductivities of 1.0 M LiPF<sub>6</sub>, 1.0 M LiBOB and 0.8 M LiBMFMB in EC-EMC (1/2 by wt.).

Fig. 2a shows the cyclic voltammograms (CVs) of a LiNi<sub>0.5</sub>Mn<sub>1.5</sub>O<sub>4</sub> working electrode in 0.8 M LiBMFMB/EC-EMC (1/2, by wt.) at a scan rate of 0.1 mV/s. In the initial anodic scan there is one minor oxidation peak at 4.24 V and one major oxidation peak at 4.84 V, corresponding to the oxidation of Mn<sup>3+</sup> to Mn<sup>4+</sup> and Ni<sup>2+</sup> to Ni<sup>4+</sup>, respectively. During the cathodic scan the two reduction peaks appear at 4.48 and 3.96 V, respectively. There are several notable changes in the second CV cycle. The first one is the shift of the minor oxidation peak to lower potential (from 4.24 V to 4.04V) and the shift of the major reduction peak to higher potential (from 4.48 V to 4.54 V), indicating the improvement of electrode kinetics with cycling. The second one is the increase of current densities for both lithium intercalation and de-intercalation at high potential, which suggests that during the initial CV cycle the electrode surface has been passivated because of the electrolyte oxidation. The third one is the appearance of the two anodic peaks corresponding to the oxidation of Ni<sup>2+</sup> to Ni<sup>3+</sup> and Ni<sup>3+</sup> to Ni<sup>4+</sup>. However, the two corresponding cathodic peaks are still overlapped because of the very narrow potential gap.<sup>22-24</sup> To better understand the above changes, the initial CVs of both LiPF<sub>6</sub> and LiBOB based electrolytes were also carried out under a scan rate of 0.1mV/s. As shown in Fig. 2b, the similar minor redox peaks between LiPF<sub>6</sub> and LiBOB indicate that the above difference observed for the LiBMFMB solution might be due to its low ionic conductivity. It is

also noted in Fig. 2b during the initial CV scan that the double anodic peaks at high potential are observed for both LiPF<sub>6</sub> and LiBOB based electrolytes. For the LiBOB based electrolyte it seems that the oxidation process, either due to the electrochemical Li<sup>+</sup> extraction or due to the oxidation of the electrolyte, has not finished at 5.0 V, as indicated by the rising current density at the end (Fig. 2b). However, during the following cycles the current densities at 5.0 V are lower than those at peaks (Fig. S2). As a comparison, the oxidation processes for both LiPF<sub>6</sub> and LiBMFMB based electrolytes are finished at 5.0 V (Fig. 2b). The higher current density at 5.0 V coupled with higher reduction potential (4.44 V) for the LiBOB based electrolyte indicates that LiBOB is less stable than LiBMFMB, as predicted by previous theoretical calculation.<sup>19</sup>

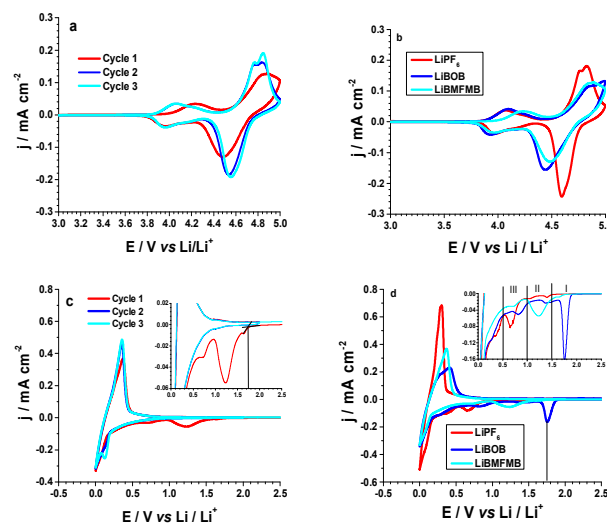


**Fig. 2.** Cyclic voltammograms of (a) LiNi<sub>0.5</sub>Mn<sub>1.5</sub>O<sub>4</sub> and (b) graphite in 0.8 M LiBMFMB/EC-EMC (1/2 by wt.) at a scan rate of 0.1mV/s. Lithium is used as both counter and reference electrode.

Fig.2c shows the CVs of a graphite working electrode in the LiBMFMB solution at a scan rate of 0.1 mV s<sup>-1</sup>. During the first CV cycle, the reduction starts at 1.75 V (see the inset), which can be attributed to the reduction of the BMFMB anion,<sup>10, 11</sup> although it is not as dominant as the BOB anion (Fig.2d). The big reduction peak at 1.2 V is clearly due to the bulk reduction of the carbonate solvents on the surface of the graphite electrode,<sup>25</sup> whereas the small peak at 0.75 V is attributed to the reduction of the solvents that are co-intercalated with lithium into the graphene layer.<sup>26-28</sup> The cathodic peak below 0.20 V and the anodic peak at 0.36 V are the typical peaks corresponding to the lithium intercalation into and de-intercalation from the graphite electrode, respectively. The reduction peaks observed in the first CV cycle disappear in the following cycles (inset of Fig. 2c), indicating the effective SEI formation on the surface of the graphite electrode. Fig. 2d compares the initial CVs of LiPF<sub>6</sub>, LiBOB and LiBMFMB based electrolytes. Clearly, the reduction processes are dramatically different because of the salt difference. Generally, each salt shows distinct reduction feature in each of the following three voltage regions, that is, I (>1.5 V), II (1.0-1.5V) and III (0.5- 1.0V) (Fig. 2d inset). For example, the conspicuous reduction peak at 1.75 V due to the reduction of the BOB anion<sup>10, 11</sup> is dominant in region I, the reduction of the LiBMFMB based electrolyte is dominant in region II, and the reduction of the LiPF<sub>6</sub> based electrolyte is dominant in region III. The CVs in Fig. 2d suggest that both LiBOB and LiBMFMB based electrolytes are reduced mainly on the surface of the graphite electrode,<sup>25</sup> although one difference is that the reduction of the BOB

anion is dominant for the former while the reduction of the carbonate solvents is dominant for the latter. For the  $\text{LiPF}_6$  based electrolyte, the reduction is mainly happened after being co-intercalated with  $\text{Li}^+$  into the graphite layers.<sup>26-28</sup> Detailed studies are needed to clarify the above differences in the future.

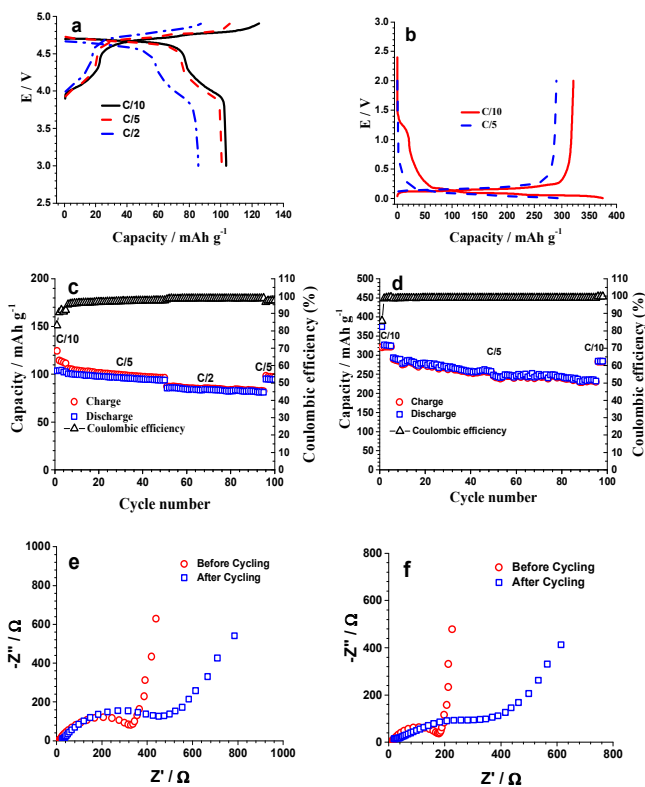


**Fig. 3.** Charge-discharge profile (a and b), cycling performance and coulombic efficiencies (c and d), and electrochemical impedance spectra (e and f) of the  $\text{LiNi}_{0.5}\text{Mn}_{1.5}\text{O}_4||\text{Li}$  (a, c and e) and  $\text{NG}||\text{Li}$  (b, d and f) half-cell using 0.8M LiBMFMB/EC-EMC (1/2 by wt.) under different current rates at room temperature.

Fig. 3a shows the charge-discharge profile of the  $\text{LiNi}_{0.5}\text{Mn}_{1.5}\text{O}_4||\text{Li}$  half-cell based on 0.8 M LiBMFMB/EC-EMC (1/2, by wt.) under different current rates at room temperature. The typical two-step charge/discharge processes are observed under all current rates. The charge (Li de-intercalation) and discharge (Li intercalation) capacities are 124.5 and 103.5 mAh g<sup>-1</sup> under C/10, 105.8 and 100.7 mAh g<sup>-1</sup> under C/5, and 87.4 and 85.7 mAh g<sup>-1</sup> under C/2, resulting in coulombic efficiencies of 83.1 %, 95.2 %, and 98.1%, respectively. The initial low coulombic efficiency is mainly due to the electrolyte oxidation under a high voltage of 4.7 V and the SEI formation on the cathode surface.<sup>9</sup> The cell exhibits good cycling stability, for example, the reversible capacities after 5 cycles at C/10, 40 cycles at C/5, and 50 cycles at C/2 are 111.5, 93.9 and 84.0 mAh g<sup>-1</sup>, respectively (Fig. 3c). The above cycling performance is much better than the half-cells based on 0.5 M LiBFMB/EC-DMC-DEC and 1.0 M LiBFMB/PC.<sup>19</sup> This is attributed to the stable structure of the LiBMFMB salt, which results in less electrolyte decomposition and thinner SEI layer. The latter is supported by the low electrochemical impedance spectroscopy (EIS) of the half-cell. As shown in Fig. 3e, the total impedance, including both the resistance of the SEI layer and that of the charge-transfer,<sup>19, 29, 30</sup> increases from 327  $\Omega$  before cycling to 474  $\Omega$  after 100 cycles. As a comparison, the total impedance of the half-cell based on 0.5 M LiBFMB/EC-DMC-DEC increased from 1028  $\Omega$  before cycling to 11084  $\Omega$  after 21 cycles

and that of the half-cell based on 1.0 M LiBFMB/PC increased from 162  $\Omega$  before cycling to 1900  $\Omega$  after 30 cycles.<sup>19</sup>

In addition to good cycling performance in the  $\text{LiNi}_{0.5}\text{Mn}_{1.5}\text{O}_4||\text{Li}$  half-cell, the new salt electrolyte also exhibits good performance in natural graphite (NG) based half-cell. As shown in Fig.3b, the charge and discharge capacities are 321 and 374.6 mAh g<sup>-1</sup> under C/10, and 289.8 and 293.8 mAh g<sup>-1</sup> under C/5, respectively. The low initial coulombic efficiency of 85.7 % is clearly due to the electrolyte reduction and the SEI formation, which is evidenced by the obvious plateau between 1.0 and 1.5 V (Fig. 3b). After the first cycle, the coulombic efficiency quickly increases to above 99.0 %, indicating the effective SEI formation (Fig. 3d). The reversible capacities after 5 cycles at C/10, and 90 cycles at C/5 are 324.3 and 230.5 mAh g<sup>-1</sup>, respectively (Fig. 3d). The good cycling performance of the  $\text{NG}||\text{Li}$  half-cell is also supported by the low EIS data. As shown in Fig. 3f, the total impedance of the half-cell is increased from 175  $\Omega$  before cycling to 370  $\Omega$  after 100 cycles.

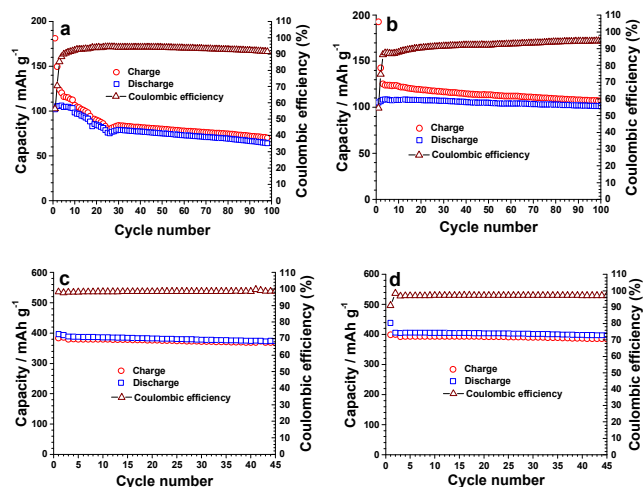


**Fig. 4.** Charge-discharge capacities and coulombic efficiencies of the  $\text{LiNi}_{0.5}\text{Mn}_{1.5}\text{O}_4||\text{Li}$  (a and b) and  $\text{NG}||\text{Li}$  (c and d) half-cells using 0.8M LiBMFMB/EC-EMC (1/2 by wt.) (a and c) and 1.0M  $\text{LiPF}_6$  / EC-EMC (1/2 by wt.) (b and d) at 60°C under different current rates (For  $\text{LiNi}_{0.5}\text{Mn}_{1.5}\text{O}_4||\text{Li}$  cell the first two formation cycles were carried out at C/5 followed by C/2 for the remaining cycles; For  $\text{NG}||\text{Li}$  cell, the first two formation cycles were carried out at C/10, followed by C/5 for the remaining cycles).

Inspired by the earlier result of better cycling performance of LiBOB based electrolyte than  $\text{LiPF}_6$  based electrolyte at high temperature,<sup>8</sup>  $\text{LiNi}_{0.5}\text{Mn}_{1.5}\text{O}_4||\text{Li}$  and  $\text{NG}||\text{Li}$  cells using both LiBMFMB and  $\text{LiPF}_6$  based electrolytes were assembled and tested at 60°C. For the  $\text{LiNi}_{0.5}\text{Mn}_{1.5}\text{O}_4||\text{Li}$  cells, the two formation cycles were carried out at a current rate of C/5, followed by C/2 for the remaining cycles. For the  $\text{NG}||\text{Li}$  cells, the first two formation cycles were carried out at C/10, followed by C/5 for the remaining cycles. Fig. 4a & b shows the cycling performance and coulombic efficiencies of the  $\text{LiNi}_{0.5}\text{Mn}_{1.5}\text{O}_4||\text{Li}$  cells based on LiBMFMB and  $\text{LiPF}_6$  electrolyte, respectively. For the LiBMFMB based cell (Fig.4a) the initial charge and discharge capacities are 181.2 and 102.0 mAh g<sup>-1</sup>, respectively, resulting in a low coulombic efficiency of 56.3%. The coulombic efficiency increases to 71% in the second formation cycle, and further increases to 85.3% when the current rate is increased to C/2. The initial reversible capacity at C/2 is 105.5 mAh g<sup>-1</sup>, which is much higher than that obtained at room temperature (Fig. 3c). Unfortunately, the capacity decreases after a few cycles, and is stabilized after 25 cycles, followed by gradual decrease with cycling. It is only 64 mAh g<sup>-1</sup> after 100 cycles. As a comparison, for the  $\text{LiPF}_6$  based cell the initial charge and discharge capacities are 193.0

and 105.3 mAh g<sup>-1</sup>, respectively, resulting in a coulombic efficiency of 54.6%. These initial low coulombic efficiencies indicate severe electrolyte oxidation happened on the surface of the cathode at high temperature, supported by the fact that the highest coulombic efficiencies achieved in both electrolytes based cells are less than 95%. However, it seems that the SEI formed in the LiPF<sub>6</sub> electrolyte is better (or thinner) than that formed in the LiBMFMB electrolyte, evidenced by the stable cycling performance. The initial discharge capacity under C/2 (the third cycle) is 108.2 mAh g<sup>-1</sup>, and it is still as high as 101.2 mAh g<sup>-1</sup> after 100 cycles. The better performance of LiPF<sub>6</sub> based cell is also supported by the EIS data. Fig. S3 reveals that the total impedance of the LiBMFMB half-cell increases from 320 Ω before cycling to 5800 Ω after 100 cycles and that of the LiPF<sub>6</sub> half-cell increases from 184 Ω before cycling to 1100 Ω after 100 cycles.

Fig. 4c & d shows the cycling performance and coulombic efficiencies of the NG||Li cells based on LiBMFMB and LiPF<sub>6</sub> electrolyte, respectively. Quite different from the results of LiNi<sub>0.5</sub>Mn<sub>1.5</sub>O<sub>4</sub>||Li, both NG||Li cells showed good cycling behavior, that is, the reversible capacities are 380 and 390 mAh g<sup>-1</sup> and coulombic efficiencies are 98.5 % and 97.2 % for LiBMFMB and LiPF<sub>6</sub> based electrolyte, respectively. The cells were stopped after 45 cycles and EIS data were measured. As shown in Fig.S3, the total impedance of the LiBMFMB based cell increases from 237 Ω before cycling to 702 Ω after 45 cycles. Even though the impedance of the LiPF<sub>6</sub> based cell is not well defined after 45 cycles, it seems that it is still less than that of the LiBMFMB based cell. Suffice to say that the good cycling performances of the two NG||Li cells are supported by the low EIS data, similar to previous report on LiBOB and LiPF<sub>6</sub> at 70°C.<sup>8</sup> The cell cycling was continued after impedance measurement and the long cycling performance as well as cell diagnosis will be reported elsewhere.

In summary, new fluorine and methyl-substituted lithium bis(2-methyl-2-fluoromalonato)borate (LiBMFMB) has been successfully synthesized. The new salt based electrolyte, 0.8M LiBMFMB in EC-EMC (1/2 by wt.), is not only compatible with the 5.0V cathode, LiNi<sub>0.5</sub>Mn<sub>1.5</sub>O<sub>4</sub>, but also compatible with the graphite anode. At room temperature, this new salt based electrolyte exhibits stable cycling performance, good rate capability, and low cell impedance in the LiNi<sub>0.5</sub>Mn<sub>1.5</sub>O<sub>4</sub> and NG based half-cells, all of which underlines the importance of replacing the acidic hydrogen in LiBFMB with the methyl group in LiBMFMB. However, when tested at 60°C, the LiNi<sub>0.5</sub>Mn<sub>1.5</sub>O<sub>4</sub>||Li cell under a current rate of C/2 exhibits fast capacity fading and large cell impedance while the NG||Li cell under a current rate of C/5 maintains good cycling performance and low cell impedance. Further analysis to identify the cause is underway.

This research was supported by the U.S. Department of Energy's Office of Science, Basic Energy Science, Materials Sciences and Engineering Division.

#### Notes and references

<sup>a</sup> Chemical Science Division, Oak Ridge National Laboratory, Oak Ridge, TN 37831, USA. \*Email: [sunx@ornl.gov](mailto:sunx@ornl.gov), Tel: 865-241-8822 Fax: 865-241-5152.

<sup>b</sup> Department of Chemistry, University of Tennessee, Knoxville, TN 37996

Electronic Supplementary Information (ESI) available: [detailed experimental section, TGA, cyclic voltammetry, electrochemical impedance spectroscopy]. See DOI: 10.1039/c000000x/

- J. W. Barthel, M.; Buestrich, R.; Gores, H. J. , *J. Electrochem. Soc.*, 1995, **142**, 2527-2531.
- J. Barthel, R. Buestrich, E. Carl and H. J. Gores, *J. Electrochem. Soc.*, 1996, **143**, 3572-3575.
- J. Barthel, M. Schmidt and H. J. Gores, *J. Electrochem. Soc.*, 1998, **145**, L17-L20.
- J. Barthel, A. Schmid and H. J. Gores, *J. Electrochem. Soc.*, 2000, **147**, 21-24.
- Germany Pat.*, DE 19829030, 1999.
- W. Xu and C. A. Angell, *Electrochem. Solid State Lett.*, 2001, **4**, E1-E4.
- V. Aravindan, J. Gnanaraj, S. Madhavi and H.-K. Liu, *Chemistry-a European Journal*, 2011, **17**, 14326-14346.
- K. Xu, S. S. Zhang, B. A. Poese and T. R. Jow, *Electrochem. Solid State Lett.*, 2002, **5**, A259.
- K. Xu, *Chem. Rev.*, 2004, **104**, 4303-4417.
- K. Xu, S. Zhang and T. R. Jow, *Electrochem. Solid State Lett.*, 2003, **6**, A117-A120.
- J. C. Panitz, U. Wietelmann, M. Wachtler, S. Stroebele and M. Wohlfahrt-Mehrens, *J. Power Sources*, 2006, **153**, 396-401.
- X. G. Sun, C. L. Reeder and J. B. Kerr, *Macromolecules*, 2004, **37**, 2219-2227.
- X. G. Sun, J. B. Kerr, C. L. Reeder, G. Liu and Y. B. Han, *Macromolecules*, 2004, **37**, 5133-5135.
- X. G. Sun and J. B. Kerr, *Macromolecules*, 2006, **39**, 362-372.
- C. Schreiner, M. Amereller and H. J. Gores, *Chem.-Eur. J.*, 2009, **15**, 2270-2272.
- P. F. Driscoll, L. Yang, M. Gervais and J. B. Kerr, *ECS Transactions*, 2011, **33**, 33-53.
- L. Yang, H. J. Zhang, P. F. Driscoll, B. Lucht and J. B. Kerr, *ECS Transactions*, 2011, **33**, 57-69.
- X. G. Sun, G. Liu, J. B. Xie, Y. B. Han and J. B. Kerr, *Solid State Ionics*, 2004, **175**, 713.
- C. Liao, K. S. Han, L. Baggetto, D. A. Hillesheim, R. Custelcean, E. S. Lee, B. K. Guo, Z. H. Bi, D. E. Jiang, G. M. Veith, E. W. Hagaman, G. M. Brown, C. Bridges, M. P. Paranthaman, A. Manthiram, S. Dai and X. G. Sun, *Adv. Energy Mater.*, 2014, **4**, 1301368 (1301361-1301312).
- X. G. Sun, C. Liao, L. Baggetto, B. K. Guo, R. R. Unocic, G. M. Veith and S. Dai, *J. Mater. Chem. A*, 2014, **2**, 7606-7614.
- M. Ding and T. R. Jow, *J. Electrochem. Soc.*, 2004, **151**, A2007-A2015.
- Q. M. Zhong, A. Bonaklarpour, M. J. Zhang, Y. Gao and J. R. Dahn, *J. Electrochem. Soc.*, 1997, **144**, 205-213.
- H. Xia, S. B. Tang, L. Lu, Y. S. Meng and G. Ceder, *Electrochimica Acta*, 2007, **52**, 2822-2828.
- T.-F. Yi and Y.-R. Zhu, *Electrochimica Acta*, 2008, **53**, 3120-3126.
- X. R. Zhang, R. Kostecki, T. J. Richardson, J. K. Pugh and P. N. Ross, Jr., *J. Electrochem. Soc.*, 2001, **148**, A1341-A1345.
- S. K. Jeong, M. Inaba, Y. Iriyama, T. Abe and Z. Ogumi, *Electrochem. Solid State Lett.*, 2003, **6**, A13-A15.
- S. K. Jeong, M. Inaba, Y. Iriyama, T. Abe and Z. Ogumi, *J. Power Sources*, 2008, **175**, 540-546.
- S. K. Jeong, M. Inaba, Y. Iriyama, T. Abe and Z. Ogumi, *Electrochimica Acta*, 2002, **47**, 1975-1982.
- S. S. Zhang, K. Xu and T. R. Jow, *Electrochem. Solid-State Letter.*, 2002, **5**, A92-A94.
- X. G. Sun and C. A. Angell, *Electrochem. Commun.*, 2009, **11**, 1418-1422.